Evaluation of underwater vehicle's self-localization based on visual odometry or sensor odometry

doi: https://doi.org/10.1109/ICIIS47346.2019.9063345

Evaluation of underwater vehicle's self-localization based on visual odometry or sensor odometry

Yoshiki Tanaka
Graduate School of Life Science and Systems Engineering
Kyushu Institute of Technology
Kitakyushu, Japan
tanaka.yoshiki732@mail.kyutech.jp

Akio Semmyo
Graduate School of Life Science and Systems Engineering
Kyushu Institute of Technology
Kitakyushu, Japan
semmyo.akio685@mail.kyutech.jp

Yuya Nishida
Graduate School of Life Science and Systems Engineering
Kyushu Institute of Technology
Kitakyushu, Japan
ynishida@lsse.kyutech.ac.jp

Shinsuke Yasukawa
Graduate School of Life Science and Systems Engineering
Kyushu Institute of Technology
Kitakyushu, Japan
s-yasukawa@brain.kyutech.ac.jp

Jyonghyon Ahn
Department of Intelligent Mechanical Engineering
Hiroshima Institute of Technology
Hiroshima, Japan
j.ahn.h2@it-hiroshima.ac.jp

Kazuo Ishii
Graduate School of Life Science and Systems Engineering
Kyushu Institute of Technology
Kitakyushu, Japan
ishii@brain.kyutech.ac.jp

***Abstract*— This research focuses on two self-localization methods for observation of the sea floor and sampling. One is a method of estimate the self-localization using Kalman filter from the acceleration data calculated from equation of motion and the velocity data considering the effect of underwater vehicle's oscillation. The other is visual odometry using a stereo camera. The AUV was deployed in a sea area 40m depth to evaluate the performance of self-localization estimated by two methods. Self-localization estimation using Kalman filter was less accurate than visual odometry, but it was confirmed that the variance of the estimated velocity was smaller than before estimation. In the visual odometry using stereo camera, it was confirmed that the estimation error depends on the travel direction of AUV and the moving direction of a stereo camera.**

***Keywords*— Sampling-AUV, self-localization, visual odometry, sensor odmetry, Kalman filter**

I. INTRODUCTION

Mineral resources and energy resources are very important basic resources in the development of industrial society, and these demands are expected to increase. There are many resources including mineral and energy resources in Japanese ocean. However, Japan depends on the import from the country that produces land resources. Therefore, it greatly depends on the political situation of the producing country to obtain resources. It is included in this cause that there are resources in the sea floor more than depth of the water 50 m that a general diver cannot go into and that neighboring environment is not clear. In recent years, ROV has been used to collect marine minerals and benthic organisms using equipped manipulators [1,2]. AUV is used for surveys that move over a wide area, such as measuring seafloor topography and surveying the distribution of biological communities[3,4]. The survey of the sea floor using an underwater vehicle does not end at once, and it is necessary to observe enviromental changes continuously. In addition, the accuracy of the survey results obtained by the vehicle greatly depends on the accuracy of it's self-localization.

In this research, we focus on self-localization to perform observation of sea floor and sampling. To improve the accuracy of self-localization, we proposed a method of self-localization estimation using Kalman filter considering the effect of vehicle's oscillation[5]. In the research of [5], the velocity was estimated using the Kalman filter from the acceleration data calculated using the equation of motion and the Doppler velocity log(DVL) velocity data. In the future, we will integrate sensor odometry and visual odometry to achieve more accurate self-localization. Therefore, we evaluated the self-localization performance to obtain the model error for these two methods. In this paper, we describe the development of a visual odometry system using a stereo camera, the evaluation of self-localization estimation using Kalman filter and a sea trial performed at 40 m depth in October 2018.

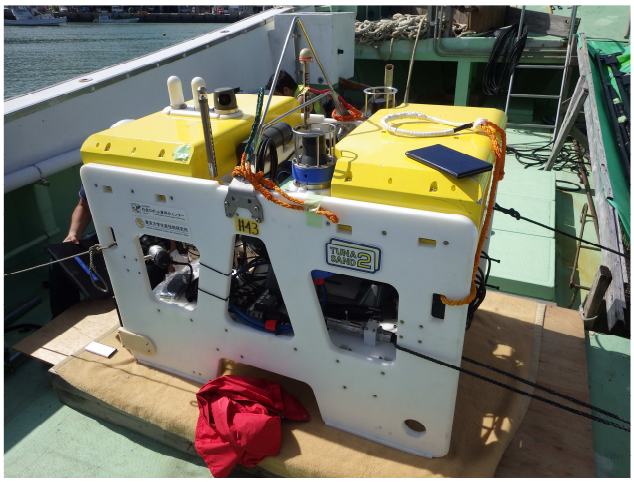

Fig.1 Appearance of Hovering type AUV Tuna-Sand2

II. SELF-LOCALIZATION METHOD FOR UNDERWATER VEHICLE

A. Platform

Fig.1 shows appearance of the AUV Tuna-Sand2. This robot is a hovering type AUV equipped with a sampling device[6-9]. Tuna-Sand2 has two pressure resistant containers called a control hull and a mapping hull. The control hull is equipped with two CPUs. One is used for navigation and the other is used for obstacle detection. This AUV has three sensors including Inertial navigation system(INS), DVL and pressure sennsor as navigation elements. The self-localization in the water is estimated using a ground velocity and altitude data from the DVL, the depth data from the pressure sensor, and true azimuth and attitude data from the INS. This AUV detects obstacles by photographing the reflected light of the sheet laser illuminating forward with the front camera. In addition, the mapping hull is equipped with a CPU. This

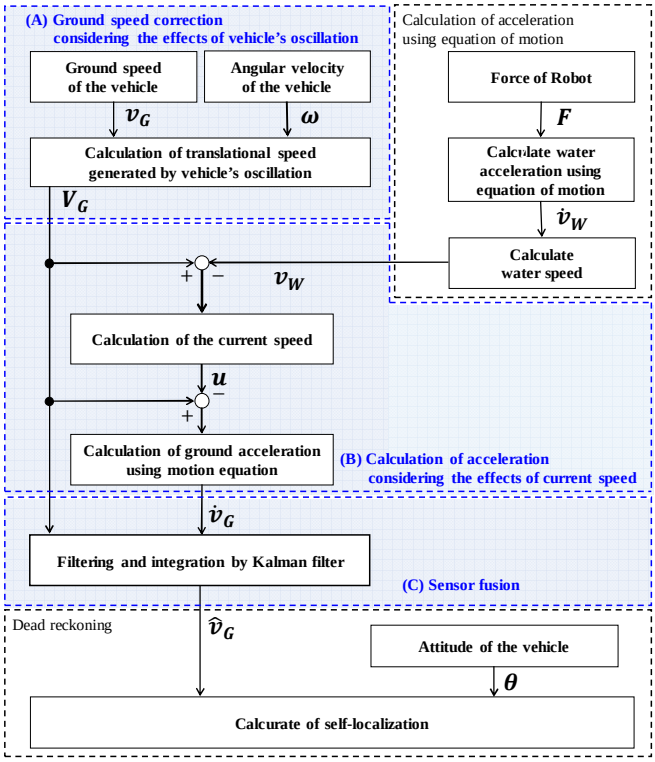

Fig.2 Self-localization method using Kalman filter

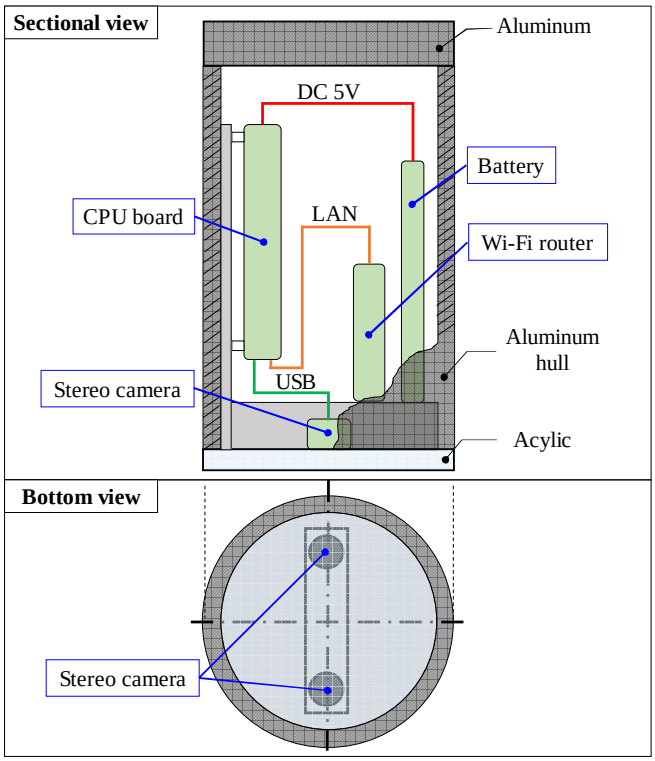

Fig.4 System configuration of Stereo camera hull

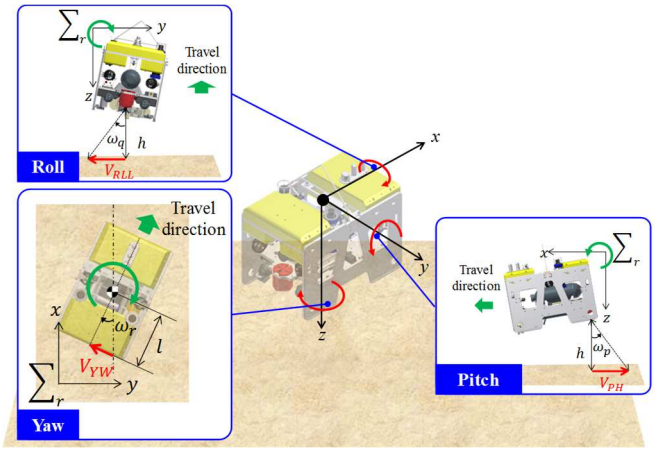

Fig.3 Translational velocity generated by the rotational motion

mapping device consists of a bottom camera, a sheet laser and two LED strobes. A three dimension mosaic image can be generated by offline processing by emitting an LED strobe and a sheet laser and taking a reflected image of the laser and seabed images.

B. Self-localization using Kalman filter

The ground velicity includes the translational velocity by underwater vehicle's oscillation as shown in Fig.3. The translational velocity V_{RLL}, V_{PH} and V_{YW} generated by the rotational movement of AUV is expressed by the following equations:

$$V_{RLL} = h \cdot \omega_p \quad (1)$$

$$V_{PH} = h \cdot \omega_q \quad (2)$$

$$V_{YW} = l \cdot \omega_r \quad (3)$$

Here, h is the altitude data from the DVL, and l is the distance from the AUV's center of gravity to the center of the DVL. As shown in Fig.2(A), we consider the effect of the underwater vehicle's oscillation by substracting the translational velocity generated by the rotational motion from the ground velocity. Therefore, the velocity V_{Gx} and V_{Gy} are expressed by the following equations:

$$V_{Gx} = v_{gx} - V_{PH} \quad (4)$$

$$V_{Gy} = v_{gy} - V_{RLL} - V_{YW} \quad (5)$$

Here, v_{gx} and v_{gy} are ground velocity data from the DVL. When estimating the acceleration using the equation of motion, the effect of the current flow is due to the motion of the robot.. Therefore, it is necessary to consider the effect of the current flow. As shown in Fig.2(B), the current flow is estimated with the velocity calculated by the equation of motion and the ground velocity measured by DVL. By assuming the effect of current flow is always applied from a certain direction during navigation, the acceleration $\dot{\boldsymbol{v}}_{\boldsymbol{G}}$ of the underwater vehicle can be expressed by the following equation:

$$\dot{\boldsymbol{v}}_{\boldsymbol{G}} = \frac{1}{\boldsymbol{M}}\{\boldsymbol{F} - \boldsymbol{D}|\boldsymbol{V}_{\boldsymbol{G}} - \boldsymbol{u}|(\boldsymbol{V}_{\boldsymbol{G}} - \boldsymbol{u})\} \quad (6)$$

Here, $\boldsymbol{M}$ is intertia matrix, $\boldsymbol{D}$ is fluid resistance coefficient matrix, $\boldsymbol{F}$ is Force of AUV, $\boldsymbol{u}$ is the current flow. Therefore, the velocity data that is input to the Kalman filter shown in Fig.2(C) includes the ground velocity data considering the effect of underwater vehicle's oscillation and the acceleration data considering the effect of the current flow. $\boldsymbol{M}$ and $\boldsymbol{D}$ are parameters estimated experimentally by limit cycle test. Then, the self-localization of underwater vehicle is estimated by transforming the estimated velocity into three axis and integrating. In this paper, a liner model expressed by the

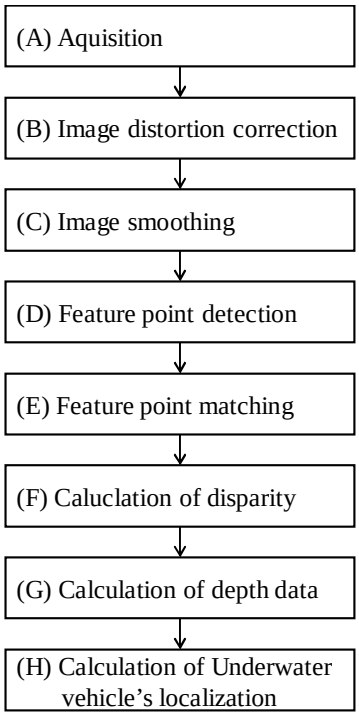

Fig.5 Processing flow of visual odmetory using stereo camera

following equation is used as the Kalman filter model [5].

$$\boldsymbol{x}(k+1) = \boldsymbol{A}(k)\boldsymbol{x}(k) + \boldsymbol{B}\boldsymbol{w_1}(k) \quad (7)$$

$$\mathbf{y}(k) = \boldsymbol{C}(k)\boldsymbol{x}(k) + \boldsymbol{w_2}(k) \quad (8)$$

$$\boldsymbol{x}(k) = [\boldsymbol{V_G}(k),\ \dot{\boldsymbol{v}}_{\boldsymbol{G}}(k),\ \boldsymbol{\omega}(k)] \quad (9)$$

Here, $\boldsymbol{x}$ is state variable, $\boldsymbol{A}$ is the state transition matrix, $\boldsymbol{C}$ is the observation matrix. The state variable $\boldsymbol{x}$ consists of velocity data, acceleration data and anguler velocity data.

C. Visual odometory system using stereo camera

Fig.4 shows the system configuration of the stereo camera module(camera hull). This camera module is mounted on the front left side of AUV Tuna-Sand2. The camera hull for photograping the sea floor is equipped with a mobile battery.This module is a stand alone device that can be mapped. The CPU board is LattePand. Stereo camera and CPU board are connected by USB cable. In addition, a CPU board and a Wi-Fi router are connected by LAN cable to prevent changes in the position and attitude of the stereo camera when the hull is opened and closed. Therefore, we can remotely control the execution a program to aquire photo-image and the confirmation of the acqired photo-image from an external PC. At first, distortion correction and smoothing processing is performed on photo-images taken with a stereo camera, and calculate two-dimensional vectors between feature points.

Fig.5 shows the processing flow of visual odometry using a stereo camera. Next, as shown in Fig.5(D) and (E), feature point are detected and matched using photo-images taken at time $t = k$ and photo-images taken at time $t = k\text{-}1$. We used Speeded Up Robust Features (SURF) to perform stable feature point detection and matching from photo-image[9]. When estimating the amount of movement of underwater vehicle using a two-dimensional vector between feature point, the distance between the camera and the feature points is generally a constant value such as altitude data from the DVL. However, in this method, the self-localization is estimated only by the data that can be aquired by the camera without using the sensor data such as DVL. Therefore, it is necessary to estimate altitude data from the image-photo. As shown in Fig.5(F), the corresponding points are searched from the left and right photo-images to estimate the disparity. When the estimated disparity is D, the distance between two cameras is b, and focal length is f, the distance z from between camera and the corresponding point is expressed by the following equation:

$$z = \frac{b \cdot f}{D} \quad (10)$$

When the horizontal angle of view is θ_w and the vertical angle of view is θ_h, the horizontal photograpy range w and the vertical photograpy range h is expressed by the following equation:

$$w = 2z \cdot \tan\frac{\theta_w}{2} \quad (11)$$

$$h = 2z \cdot \tan\frac{\theta_h}{2} \quad (12)$$

Here, z is the distance between the camera and the feature point. If the two-dimensional vectors between feature points obtained using SURF are d_{px} and d_{py}, the amounts of movement of camera dx and dy are expressed by the following equation:

$$dx = d_{px} \cdot \frac{w}{S_w} \quad (13)$$

$$dy = d_{py} \cdot \frac{h}{S_h} \quad (14)$$

Here, S_w and S_h are the image sizes in the horizontal and vertical directions. In this paper, we set it to 640×480 pixels. The result of movement shown in Fig.5(H) depends on the number of matched feature points. Therefore, we estimated the self-localization by using the average value as the amount of movement of the underwater vehicle.

III. SEA TRIALS

For evaluating the performance of a self-localization using Kalman filter and visual odometry, we collected basic data of sensors mounted the AUV and photo-image taken with a stereo camera The hovering type AUV Tuna-Sand2 was deployed at the depth of 40 m, and tracked waypoints at a constant velocity and altitude. Fig.6 shows the path planning for AUV Tuna-Sand2. After reaching the sea floor, the AUV cruised along the waypoint at 0.1 m/s and 1.5 m altitude. In addition, the sea floor was taken every 1.5 second using a stereo camera. In this sea trial, the true azimuth angle of AUV was constant. For evaluating the performance of self-localizaion, we set landmarks on the images taken at the observation point shown in Fig.5.

Fig.7 shows waypoints and the sef-localization of AUV calculated based on the INS data. During cruising along the waypoint, the AUV mednders with position control within an error of 0.5 m.

Fig.8(a) and (b) photo-images taken by the AUV at the each observation point (A to H) and the position of the feature points of each photo-images calculated based on INS data and

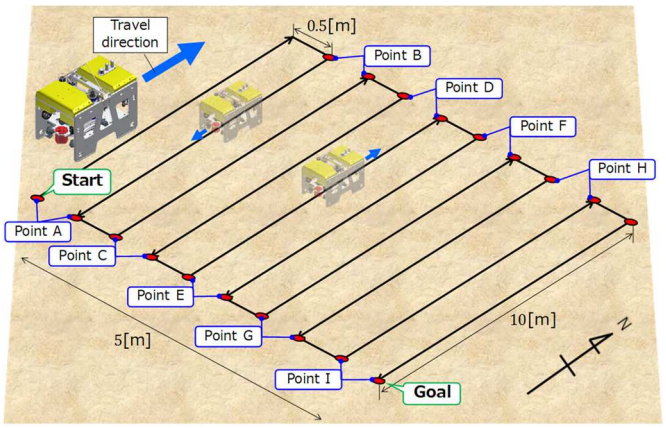

Fig.6 Path planning for Tuna-Sand2

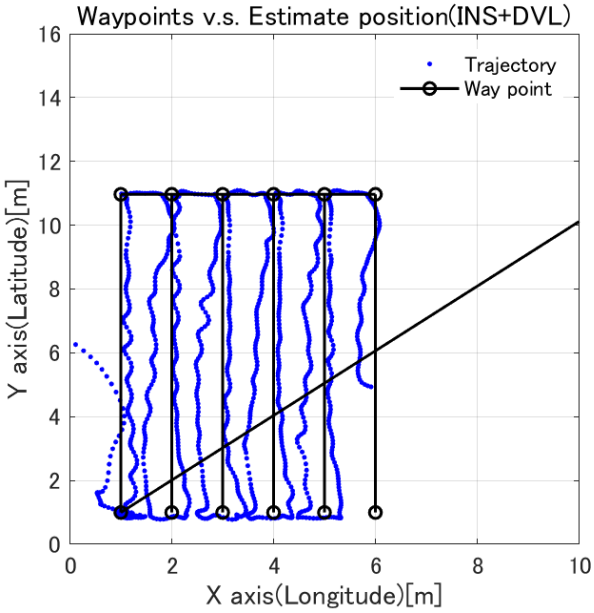

Fig.7 Movement trajectory of AUV Tuna-Sand2

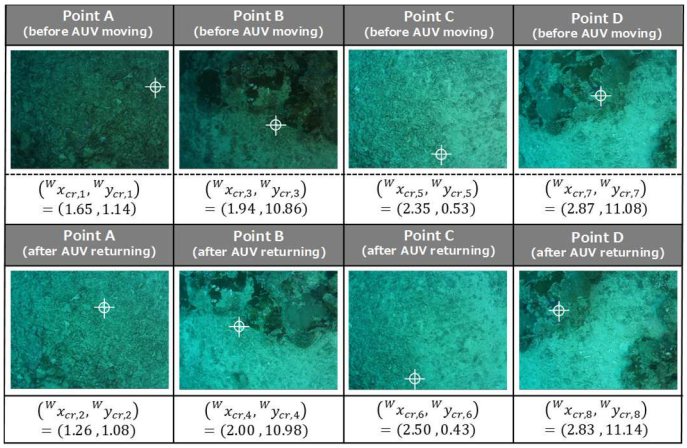

(a)

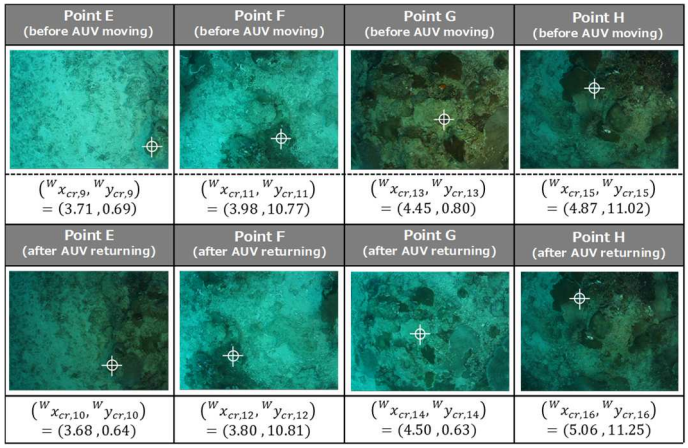

(b)

Fig.8 (a)Photo-images from observation points A to D. (b)Photo-images from observation points E to H.

Eq.(13) and Eq.(14). Fig.8(a) shows photo-images taken at observation points A to D. Fig.8(b) shows photo-images taken at observation points E to H. In Fig.8(a) and (b), the upper part is photo-images taken each observation points before the AUV moving, and lower part is photo-images after the AUV returning. $({}^{w}x_{cr,i}, {}^{w}y_{cr,i})$ is absolute position of the feature point as seen from the robot at each observation points.Table 1 to Table 3 show east-west direction error, north-south direction error and distance error at the observation points.

The self-localization based on the velocity data considering the effect of the underwater vehicle's oscillation included 0.086 m average error in the east-west direcion and 0.115 m average error in the north-south direction. It can confirmed that the distance error is smaller than the self-localization based on the DVL velocity data. Therefore, it is effective to improve the self-localization accuracy to consider the effect of the underwater vehicle's oscillation.

The self-localization using Kalman filter included 0.434 m average error in the east-west direction and 0.294 m average error in the north- south direction. As a result of comparison with the self-localization based on the DVL velocity data, the estimation method based on the velocity data estimated using Kalman filter could not contribute to the improvement of the self-localization accuracy. The reason for this is that errors are included in the actual robot behavior and model of motion of equations. However, as shown in Fig.9, the velocity data estimated by the Kalman filter has a variance of 5.74×10^{-4} for the target velocity, and it can be confirmed that it is smaller than the variance 7.39×10^{-4} of the velocity data from DVL. Therefore, the noise contained in the velocity data could be suppressed by applying the Kalman filter to the DVL velocity data.

Visual odometry using a stereo camera included 0.257 m average error in the east-west direction and 0.073 m average error in the north-south direction. Compared with the self-localization based on the DVL velocity data, the average error in the north-south direction was smaller. Therefore, the self-localization accuracy has improved. However, the average error was large in the east-west direction. This is related to the direction of the stereo camera and the travel direction of the AUV. The overlapping area of two photo-images differ depending on whether the baseline between the cameras is vertical or horizontal with respect to the direction of travel of Tuna-Sand2. The accuracy of stereo matching depends on the overlapping areas of the photo-images. Therefore, the average

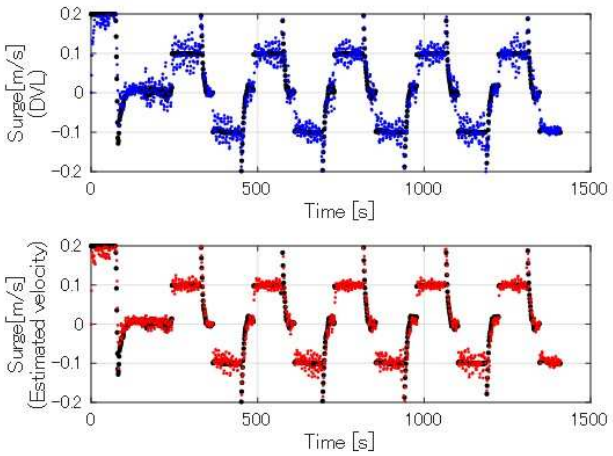

Fig.9 Comparison of velocity data from the DVL and velocity data estimated by Kalman filter against target velocity.

error increased in the east-west movement with few overlapping areas.

IV. CONCLUSION

In this paper, we proposed a visual odometry system using a stereo camera. We also reported the results of sea trials conducted in October 2018 to evaluate the performance of self-localization. Then, we introduced a method of self-localization using Kalman filter considering the effect of underwater vehicle's oscillation, and compared it with visual odometry. As a result, the self-localization calculated based on the velocity data estimated by Kalman filter ws less accurate than the visual odometry using a stereo camera. However, the estimated velocity data variance was smaller than the DVL velocity data. In visual odometry, it was confirmed that the average error of the self-localization greatly changed depending on the travel direction of AUV.

In the future, we reconstruct the motion model to reduce the error of the AUV's actual behavior and motion model and investigate a more accurate self-localization method by integrating the self-localization estimated based on sensor data and visual odometry.

TABLE I. POSITION ERROR OF EAST-WEST DIRECTION AT EACH OBSERVATION POINT

Observation Point	Position error of east-west direction [m]			
	Simple D.R.	Correct D.R.	Kalman D.R.	Visual Odometory
A	0.002	0.041	0.407	0.423
B	0.043	0.057	0.183	0.373
C	0.074	0.100	0.115	0.147
D	0.041	0.120	0.410	0.276
E	0.027	0.007	0.503	0.230
F	0.147	0.162	0.704	0.275
G	0.153	0.114	0.717	0.073
H	0.023	0.038	0.417	0.178

TABLE II. POSITION ERROR OF NORTH-SOUTH DIRECTION AT EACH OBSERVATION POINT

Observation Point	Position error of north-south direction [m]			
	Simple D.R.	Correct D.R.	Kalman D.R.	Visual Odometory
A	0.049	0.143	0.226	0.069
B	0.238	0.102	0.468	0.090
C	0.074	0.188	0.245	0.152
D	0.218	0.067	0.269	0.071
E	0.065	0.055	0.178	0.002
F	0.079	0.161	0.473	0.007
G	0.286	0.087	0.197	0.123
H	0.244	0.018	0.369	0.184

TABLE III. POSITION ERROR OF DISTANCE AT EACH OBSERVATION POINT

Observation Point	Position error of Distance [m]			
	Simple D.R.	Correct D.R.	Kalman D.R.	Visual Odometory
A	0.049	0.149	0.465	0.429
B	0.242	0.117	0.502	0.384
C	0.105	0.213	0.271	0.211
D	0.222	0.138	0.490	0.285
E	0.071	0.056	0.534	0.230
F	0.167	0.228	0.848	0.275
G	0.324	0.143	0.743	0.143
H	0.245	0.042	0.557	0.256

REFERENCES

[1] C.E. Fitzgerald, K.M. Gillis, Hydrothrmal Manganese Oxide Deposits from Baby Bare Seamount in the Northeast Pacific Ocean, Marine Geology, Vol.225, Issue 1-4, pp.145-156,2006

[2] S. Thatje, S.Hall, C.Hauton, C.Held and P. Tyler, Encounter of Lithodid Crab Paralomis Birsteini on the Continental Slope off Antarctica, Sampled by ROV, Polar Biology, Vol.31, Issue 9, pp.1143-1148, 2008

[3] Y. Nishida, K. Nagahashi, T. Sato, A. Bodenmann, B. Thornton, A. Asada and T. Ura, Development of an autonomous underwater vehicle for survey of cobalt-rich manganese crust, OCEANS2015 MTS/IEEE Washington, pp.1-5, 2015

[4] B. Thorton, A. Bodenmann, O. Pizarro, S.B. Williams, A. Friedman, R. Nakajima, K. Takai, K. Motoki, T. Watsuji, H. Hirayama, Y. Matsui, H. Watanabe and T.Ura, Biometric assessment of deep-sea vent megabenthic communities using multi-resolution 3D image reconstructions, Deep Sea Research Part I: Oceanographic Research Papers, Vol.116, pp.200-219, 2016

[5] Y. Tanaka, Y. Nishida, J. Ahn and K. Ishii, Underwater vehicle localization considering the effects of its oscillation, 2019 IEEE Underwater Technology, 2019

[6] Y. Nishida, T. Sonoda, S. Yasukawa, J. Ahn, K. Nagano, K. Ishii and T. Ura, Underwater Platform for Intelligent Robotics and its Application in Two Visual Tracking Systems, Journal of Robotics and Mechatronics, Vol.30, No.2, pp.238-247, 2018

[7] S. Yasukawa, J. Ahn, Y. Nishida, T. Sonoda, K. Ishii and T. Ura, Vision system for an autonomous underwater vehicle with a benthos sampling function, Journal of Robotics and Mechatronics, Vol.30, No.2, pp.248-256, 2018

[8] J. Ahn, S. Yasukawa, T. Sonoda, Y. Nishida, K. Ishii and T. Ura, An Optical Image Transmission System for Deep Sea Creature Sampling Missions Using Autonomous Underwater Vehicle, IEEE Journal of Oceanic Engineering, pp.1-12, 2018

[9] Y. Nishida, T.Sonoda, S. Yasukawa, J. Ahn, K. Watanabe, K. Ishii and T. Ura, Benthos Sampling by Autonomous Underwater Vehicle Equipped a Manipulator with Suction Device, 2019 IEEE Underwater Technology, 2019

[10] Herbert Bay, Tinne Tuytelaars, Luc Van Gool, SURF:Speeded Up Robust Features, computer vision-eccv lecture notes in Computer Science, pp.404-417, 200